analytical chemistry

pubs.acs.org/ac Article

Shake It Off! Acoustic Manipulation of Lipid Vesicles for Mass Spectrometric Analysis

Ashton N. Taylor, Yuqi Huang, Cheyenne Sircher, Sandra Khalife, Venkat Bhethanabotla, and Theresa Evans-Nguyen*

Cite This: *Anal. Chem.* 2023, 95, 13497−13502 Read Online

ACCESS | Metrics & More | Article Recommendations | Supporting Information

ABSTRACT: Analyzing lipid assemblies, including liposomes and extracellular vesicles (EVs), is challenging due to their size, diverse composition, and tendency to aggregate. Such vesicles form with a simple phospholipid bilayer membrane, and they play important roles in drug discovery and delivery. The use of mass spectrometry (MS) allows for broad analysis of lipids from different classes; however, their release from the higher order structural aggregates is typically achieved by chemical means. Mechanical disruption by high frequency surface acoustic waves (SAW) is presented as an appealing alternative to preparing lipid vesicles for MS sampling. In this work, SAWs used to disrupt liposomes allow for the direct analysis of their constituent lipids by employing SAW nebulization with corona discharge (CD) ionization. We explore the effects of duration, frequency, and incorporation of nonpolar lipids, including cholesterol, on the SAW's ability to disrupt the liposome. We also report on the successful MS analysis of liposome-derived lipids along with cytochrome C in solution, thus demonstrating applications to aqueous samples and native MS conditions.

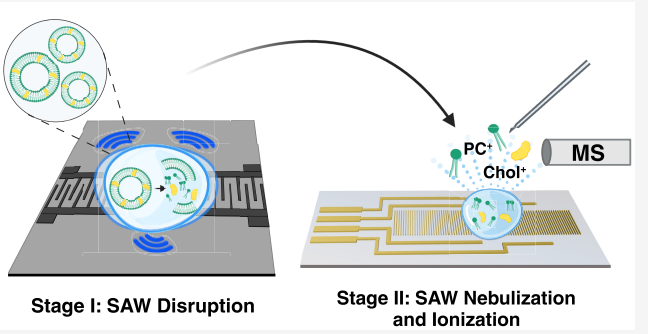

INTRODUCTION

Lipid vesicles are molecular constructs that appear widely in the biomedical field. For instance, synthetic lipid nanoparticles known as liposomes are commonly used as drug-delivery vehicles.[1] Meanwhile, naturally occurring extracellular vesicles (EVs) are of increasing interest as disease biomarkers.[2] Compositional analysis of lipid vesicles is unfortunately complex, with a diversity of lipids. Polar and nonpolar lipids require different optimal extraction and separation methods and even ionization sources for mass spectrometric analysis.[3] Liposome's customizability in composition and cargo allows for the ability to mimic EVs. Previous work by Frick et al. shows liposomes are capable of carrying membrane proteins, which makes liposomes ideal candidates as models for exosomes.[4,5] While organic solvents and detergents commonly help to disrupt these lipid nanostructures, such conditions may be inherently denaturing to vesicle cargo, including proteins.[6] Furthermore, significant nonpolar lipid composition, such as cholesterol, hinders conventional electrospray ionization (ESI) that varies with the solvent environment. Several factors, including lipids' polarity, acyl chain length, and degree of saturation, affect critical micelle concentration, which likely affects aggregation that subsequently induces matrix effects in ESI.[7,8] Therefore, a means of mechanical handling may permit the maintenance of an aqueous chemical environment amenable to sampling both liposomal lipids and proteins.

In previous work, Song et al. reported on a broadband atmospheric pressure chemical ionization source that leveraged acoustic nebulization and corona discharge to sample both polar and nonpolar analytes.[9,10] Additionally, Bhethanabotla and co-workers previously discerned the use of surface acoustic waves (SAWs) to disrupt nonspecific binding of proteins.[11,12] Therefore, the application of SAWs could demonstrate potential utility in both lipid vesicle disruption and lipid ionization. Already in the literature, Taller et al. described the microscale use of SAWs to lyse EVs and characterized the process by changes in particle size distribution.[13] Currently, in a more bottom-up approach, we employed SAWs to similarly disrupt lipid vesicles and instead characterize the process by their molecular composition in mass spectrometry.

Liposomes of a uniform size distribution served as model lipid vesicles with a single lipid bilayer.[14] Simple liposome compositions consist of primarily dioleoylglycerophosphocholine (DOPC) with a fraction of cholesterol. Liposomes are also studied in mixtures with a protein and a lipid standard, added externally in a nonvesicle form. To distinguish two discrete

Received: April 20, 2023
Accepted: August 17, 2023
Published: August 30, 2023

https://doi.org/10.1021/acs.analchem.3c01722
Anal. Chem. 2023, 95, 13497−13502

functions, SAWs are applied in two modalities: one to disrupt the liposome macrostructure and a second to nebulize solution components for subsequent corona discharge ionization. We first validate that the commercial surface acoustic wave nebulization (SAWN), enhanced with corona discharge (CD), achieves satisfactory detection of polar and nonpolar lipids simultaneously. Following this demonstration, we investigate custom-built high-frequency (>10 MHz) SAW devices to establish operational parameters that achieve liposome disruption. We finally show the simultaneous detection of protein and liposome-derived phospholipids in a primarily aqueous solution. In this manner, the systematic use of acoustics exhibits the potential to aid mass spectral analysis in native applications of both lipids and proteins.

EXPERIMENTAL SECTION

Chemicals. LC/MS grade water and methanol were purchased from Fisher Scientific (Fair Lawn, NJ). Lipids in both solution and solid form, including 1,2-dioleoyl-*sn*-glycero-3-phosphocholine (DOPC), 1,2-dioleoyl-*sn*-glycero-3-phosphocholine (DOPE), 1,2-dipalmitoyl-*sn*-glycero-3-phosphocholine (DPPC), and cholesterol, were acquired from Avanti Polar Lipids (Birmingham, AL). Cytochrome C (Fischer Scientific) was prepared in water with 10 mM ammonium acetate (Millipore Sigma).

Liposome Preparation. DOPC-only liposomes were synthesized in-house using established methods of thin-film hydration and extrusion.[15,16] DOPC-cholesterol liposomes, ∼100 nm in size, were synthesized in a similar fashion to contain 2.5, 10, and 40 mol % cholesterol. Briefly, solutions of 1 mg/mL DOPC in chloroform are evaporated in a 25 mL round-bottom flask under vacuum using a Buchi Rotavapor R-200. After drying to a lipid film, water was added to hydrate and maintain the desired concentration. The suspension was agitated on the rotary evaporator for 2 h and then bath-sonicated until translucent to form multilamellar vesicles. Vesicles were downsized over 11 passes through an extruder (Avanti Polar Lipids) with 100 nm polycarbonate membranes (Whatman) to produce ∼100 nm unilamellar liposomes. Following dilution and filtration, dynamic light scattering (Zetasizer Nano from Malvern Instruments and NanoBrook from Brookhaven Instruments) was used to measure the average hydrodynamic radius of the liposomes from ∼130 μL sample volumes. Particle size averages, obtained at 25 °C, were found to be ∼95−115 nm for all liposomes. Subsequent liposome stock solution at 1 mg/mL was diluted to concentrations 1.56−127 μM in LC/MS grade water for SAW interrogations. All liposome solutions are reported in terms of formal lipid concentrations for clarity. Liposome solutions are spiked with internal standards (DOPE, DPPC) or cytochrome C, prepared in 1:99 (v/v) methanol/water with 10 mM ammonium acetate and vortexed prior to disruption (Scheme S1).

Internal Standard Calibrator Formulation. Calibrator solutions of DOPC and DOPE lipids were formulated as formal concentrations in 1:99 methanol/water solutions to mimic the ultimately aqueous environment of the liposomes (Scheme S1). The calibrator concentrations were chosen to be 5−60 μM DOPC and 50 μM DOPE. The working concentrations were chosen taking into account reported critical micelle concentration (CMC) of each lipid. Reported CMC values for similar class lipids in water are considerably low, in the nanomolar range.[17] Based on the trends for longer acyl chain length in water and the kinetics of phospholipids spontaneously aggregating at high concentrations, these particular lipids are most likely aggregated under these conditions.[18−21] We also adopted more "native" aqueous solution conditions by incorporating ammonium acetate to facilitate the dissolution of the lipids and ultimately ionization. Explicit preparation steps for these solutions are included in the Supporting Information (Scheme S1).

Mass Spectrometer. MS analysis was performed on a linear ion trap mass spectrometer (LTQ XL, Thermo Scientific, San Jose CA) in positive ion mode. The maximum in-source fragmentation of 100 V was necessary for additional desolvation and increased signal detection. Acquisition parameters of a 200 ms maximum inject time and three microscans were set. The onboard syringe pump used in direct infusion mode provided all continuous mode sampling.

Ionization Methods. The SAWN setup, including the power supply (SAWN controller 2.0) and 9.56 MHz standing wave chips, was purchased from Deurion LLC (Seattle, WA). In droplet-mode, samples of typically 1 μL were placed in the center of the chip and rapidly nebulized at 8.25 W. To enhance ionization efficiency, a corona discharge source was assembled from the standard commercial atmospheric pressure chemical ionization (APCI) needle connected to an external high voltage power supply (PS350, Stanford Research System, Sunnyvale, CA). The APCI needle was placed in series with a 6 kΩ current limited resistor and a 60 μH inductor. The voltage supplied to the needle was set to +3.4 kV and current-limited to 1 μA. The SAWN chip was positioned 5 mm below the ion transfer tube of the MS whereas the APCI needle was positioned 7 mm away. For continuous-mode SAWN-APCI, depicted in Figure S1, a sample solution was supplied at a flow rate of 25 μL/min through PEEK tubing oriented above the center of the SAWN chip. Likewise for ESI, sample solution was supplied with a flow rate of 25 μL/min, through a 75 μm emitter at +3.4 kV.

SAWs Used for Disruption. For liposome solutions, the commercial Deurion SAWN device of 9.56 MHz was adapted to include a period of disruption using a lower applied power of ∼1 W followed by the nebulization step conducted at the higher power of 8.25 W. Additional SAW devices for liposome disruption were fabricated on a 4 in. 128° YX lithium niobate substrate. The two regions of interdigitated transducers (IDTs) on the SAW devices are designed with periodicities of 240, 120, 60, and 40 μm, in order to generate center frequencies at approximately 16.3 32.7, 65.3, and 98 MHz. The IDT regions were fabricated using standard photolithography. First, NR9 1500PY (Futurrex) negative photoresist was spin-coated on cleaned $LiNbO_3$ wafer to achieve a thickness of 2 μm. Then after UV light exposure using a Karl Suss mask aligner and baking, the pattern was developed and followed by 10 nm/100 nm Cr/Au metal layers using e-beam evaporation. Remaining metal was removed using an acetone bath, and the wafer was subsequently diced into 2 cm × 2 cm chips.

For custom-fabricated SAW devices to achieve liposome disruption, an input signal at the center frequency was generated with an RF signal generator (Rohde & Schwarz SMA100A) and coupled with an RF amplifier (Mini-Circuits LZY-22+). The RF signal between the two IDTs results in Rayleigh wave formation along the piezoelectric surface. Propagation of these waves into the liquid sample droplet achieves acoustic streaming. All custom chips were operated at 1 W. Discrete 7 μL droplets of liposome solution were exposed

https://doi.org/10.1021/acs.analchem.3c01722
Anal. Chem. 2023, 95, 13497−13502

to the low-power disruption mode for 10−60 s prior to MS analysis by SAWN-APCI.

RESULTS AND DISCUSSION

Demonstrated Application of SAWN-APCI to Lipids. We first established that baseline detection could be achieved with SAWN-APCI of specific polar and nonpolar membrane lipids in solution, as done for other targets in prior work. Prototypical membrane lipids, DOPC and cholesterol, were analyzed together as an organic solution using a continuous microflow mode for direct comparison of SAWN-APCI to ESI. In Figure 1, mass spectra depict clear DOPC ionization for

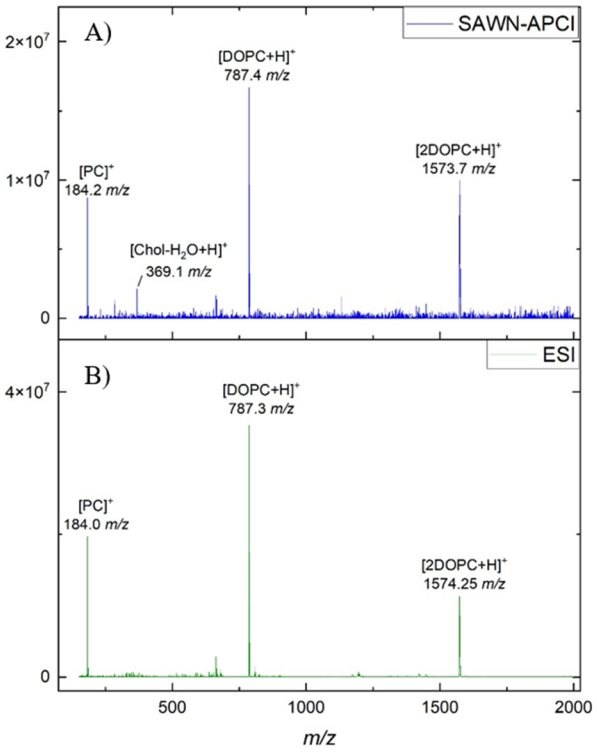

Figure 1. Prototypical lipids from lipid vesicles were evaluated in inorganic solutions by using (A) SAWN-APCI and (B) ESI. A spectrum of 50 μM DOPC and 12.5 μM cholesterol in 10 mM ammonium acetate methanol/chloroform at 4:1 at 25 μL/min.

both SAWN-APCI and ESI with comparable signal intensity, though greater noise is seen in SAWN-APCI. DOPC is represented by the protonated monomer $[DOPC + H]^+$, the protonated dimer $[2DOPC + H]^+$, and the phosphocholine headgroup $[PC]^+$, a commonly observed fragment.[22] While cholesterol exhibits poor ionization efficiency by ESI, it is visibly represented in the SAWN-APCI spectrum as the molecular ion, but more prominently in the form of a water loss $[Chol\text{-}H_2O + H]^+$ at 369.1 m/z.[23] The relative intensity of cholesterol, when normalized to total DOPC signal, was ∼5% and ∼1% for SAWN-APCI and ESI, respectively. We suspect that in addition to the physical volatilization of analyte species, the applied acoustic forces break up microscopic lipid aggregates to achieve better ionization efficiency. Anecdotally, the narrow-bore ESI emitter capillary clogged repeatedly, requiring frequent disassembly and cleaning of both the emitter and the ion inlet. Thus, the continuous microflow SAWN-APCI may be relatively more practical than ESI in the study of lipids.

Optimization of SAW Disruption of Liposomes. We hypothesized that the SAW operation could be deliberately used to disrupt lipid aggregates and release individual lipid components. We thus adopted liposomes as an initial model, providing controlled lipid composition and size. A multipass lipid extrusion process, performed in-house, provided synthetic unilamellar liposome vesicles ∼100 nm in diameter. Liposome solutions were first investigated at a formal concentration of 127 μM DOPC in water as droplet volumes of 7 μL applied to the SAW chips. Relatively low power SAWs (∼1 W) were studied at a series of disruption frequencies using the commercial SAWN device (9.56 MHz), as well as custom-fabricated SAW chips: 16, 32, 64, and 98 MHz. Exposure to the disruption frequency was conducted for 0, 10, 20, 30, 40, and 60 s. Subsequently, 1 μL aliquot droplets were then transferred to the commercial SAWN-APCI chip to be nebulized in the discrete droplet mode. Representative mass spectra of the liposome-derived lipids feature monomer and dimer DOPC ions (Figure S2). In Figure 2, the extracted ion

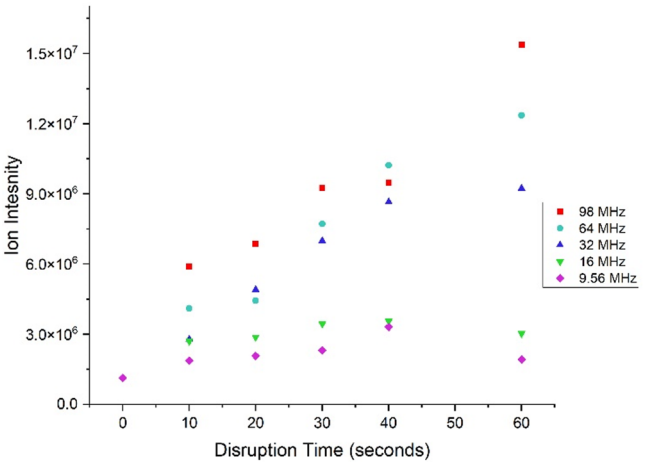

Figure 2. Liposomes of ∼100 nm diameter (127 μM DOPC) in water were subjected to varying frequencies and durations of SAW disruption parameters.

intensities of these two ions are shown for the various frequencies with respect to the disruption exposure time. It is noted that without a deliberate disruption phase (i.e., 0 s), the SAWN-APCI alone yields poor lipid signal-to-noise. Generally, higher frequencies and longer exposure times result in greater DOPC signal intensity. In releasing individual lipids from the macro-structure of the 100 nm liposomes, the acoustic methods employed generally provide lipid signal proportionate with frequency and time. Cursory SAW parameters for disruption of 100 nm DOPC liposomes yielded the highest observed signals in the range of 30−60 s. While 98 MHz yielded the highest ion intensity, the chips were more susceptible to cracking. Characteristic thermal conditions of SAW disruption are reported for various chips using infrared imaging in Table S1 and Figure S3. SAW chips at 64 MHz were subsequently chosen for their resilience and satisfactory ion signal and were used for further disruption experiments.

At this point, we also incorporated ammonium acetate into the aqueous solvent, which facilitated ionization at lower concentrations. To investigate particle concentration detection limits, liposomes were further studied at dilutions from 1.6 to 25 μM DOPC disrupted for 40 s at 64 MHz. In Figure 3, ion

https://doi.org/10.1021/acs.analchem.3c01722
Anal. Chem. 2023, 95, 13497−13502

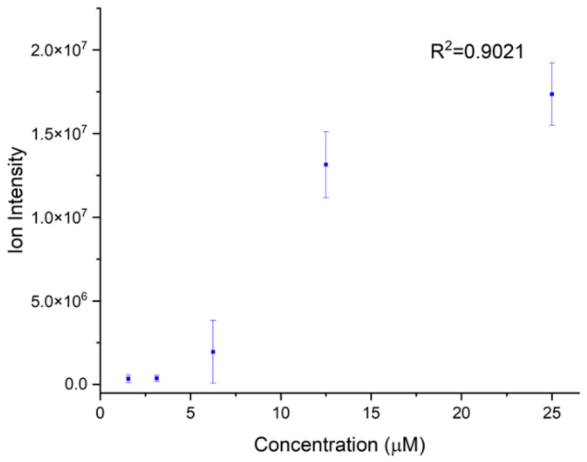

Figure 3. DOPC liposomes ranging in concentrations from 1.56 to 25 μM DOPC liposomes ion intensity after being exposed to 64 MHz for 40 s.

signal from DOPC was observed down to 1.6 μM DOPC or $\sim 11 \times 10^6$ liposomes/μL. At this low concentration, the ion intensity of the PC headgroup, along with DOPC's monomer and dimer, including sodium adducts, were all visible (Figure S4). Interestingly, the nonlinear relationship of signal to concentration would indicate some self-matrix effect of DOPC across the combined use of SAW disruption and SAWN-APCI.

Binary Mixtures. To more quantitatively determine the lipid release from liposomes, we attempted to measure the released DOPC by including an internal standard. In Figure 4,

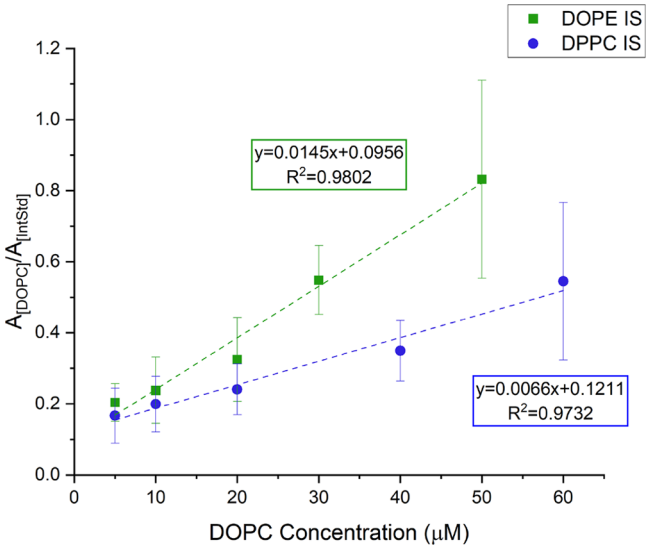

Figure 4. Two DOPC lipid calibration curves from 5 to 60 μM, using each 50 μM DOPE and 25 μM DPPC as an IS.

a calibration curve spans formal DOPC concentrations ranging from 5 to 50 μM, for which each solution was spiked with 50 μM DOPE or 25 μM DPPC. Using SAWN-APCI alone, signals were collected for multiple discrete 1 μL droplets for each of the calibrator solutions (Figure S5). The relative ionization efficiency of the lipids DOPC to DOPE and DPPC results in signal response factors of ~0.84 and ~0.5, respectively. While the calibrators comprise formal lipid concentrations, we note that the extent of lipid aggregation and truly free lipids is unknown in these primarily aqueous solutions. DOPE exhibits greater ionization efficiency than DOPC, but as the DOPC concentration increases, the error increases, reflecting a matrix effect due to a lower DOPE signal. We speculate that rising lipid content in water facilitates DOPC microscale aggregation with DOPE in solution at the formal concentrations studied. In the case of DPPC, similar behavior is observed but more dramatic due to a wider difference in ionization efficiency. Nonetheless, in either case, a linear calibration curve was established to assess the level of DOPC released by liposome disruption amidst the spiked internal standards.

The use of DPPC as an internal standard to study the release of DOPC from liposomes was evaluated but yielded complex spectra (Figure S6). We subsequently focused on the DOPE internal standard to quantify the release of DOPC from the liposomes while also studying the incorporation of cholesterol into the DOPC envelope. A series of liposome formulations was produced with the same total lipid concentration of 15 μM (DOPC + cholesterol) featuring 0, 2.5, 10, and 40 mol % of cholesterol. Liposomes (100 nm, 15 μM) underwent exposure to 64 MHz SAWs for 30−60 s and were then transferred in 1 μL aliquots to SAWN-APCI for MS analysis. In Figure 5, a

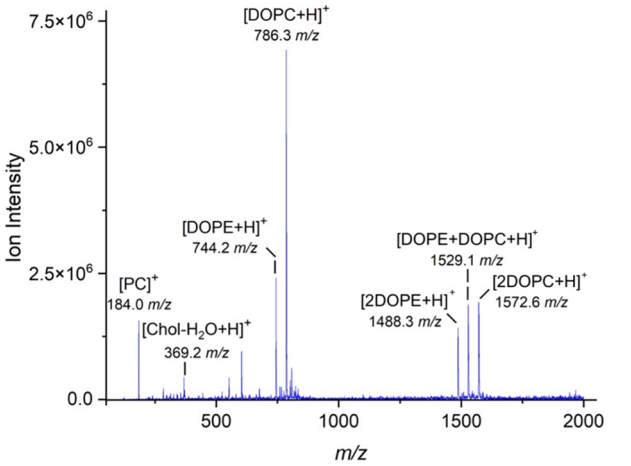

Figure 5. Liposomes comprised of 10% cholesterol at 15 μM total lipid were spiked with 50 μM DOPE IS, exposed to 60 s of 64 MHz SAW disruption.

sample mass spectrum is shown of 10% cholesterol liposomes, spiked with 50 μM DOPE, subjected to 60 s disruption. Interestingly, the released DOPE signal appears to be relatively suppressed compared to released DOPC. Additionally notable is the fact that a heterologous dimer of DOPC and DOPE (1529.1 m/z) is comparable to that of the dimers of DOPE (1488.3 m/z) and DOPC (1572.6 m/z). Therefore, immediately following the disruption phase, individual DOPC released from the liposome readily associates with the spiked DOPE, suggesting the formation of a mixed aggregate in solution.

Cholesterol is generally viewed as adding rigidity to bilayer membranes, making them more robust against disruption.[24] Toward characterizing this phenomenon, Figure 6 depicts the observed DOPC released (after 30 and 60 s disruptions) across representative cholesterol incorporation that may be observed in biological membranes. Using the prior DOPE/DOPC calibration curve, the cholesterol-free liposome study at 0% shows little difference between the two disruption durations, suggesting an efficient disruption. However, closer inspection reveals an overly strong DOPC/DOPE signal yielding an

https://doi.org/10.1021/acs.analchem.3c01722
Anal. Chem. 2023, 95, 13497−13502

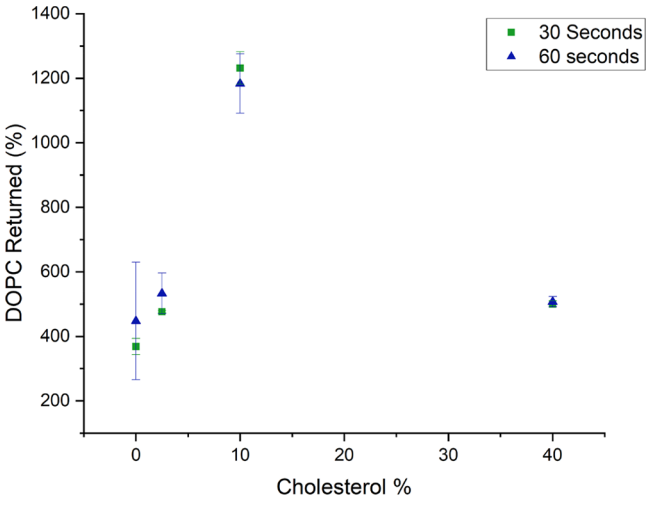

Figure 6. Liposomes composed of 15 μM total lipid are analyzed with varying cholesterol content: 0, 2.5, 10, and 40% cholesterol, each spiked with 50 μM DOPE IS.

unbelievably high recovery (350−450%). Therefore, even without cholesterol, we may surmise that the presence of the DOPC in liposome formation suppresses DOPE signal through reaggregation, such as the fresh formation of mixed micelles or possibly incorporation of DOPE into incompletely disrupted liposomes.

From 2.5% to 10% cholesterol, quantified DOPC increases, despite smaller formal concentrations of DOPC. At 10% cholesterol content, longer disruption yields the highest overall measurement of DOPC, but notably low and inconsistent cholesterol signal (Figure S7). The 1230% recovery stands out, demonstrating that cholesterol has an outsized matrix effect on the overall method. Quantitation of the cholesterol itself is complicated due to its >100 times lower solubility in water than the phospholipids while the purported CMC of cholesterol is in the nM range.[25] Consequently, it is reasonable that any released cholesterol may also rapidly reaggregate with both released DOPC and spiked DOPE during the transfer of the droplet to the SAWN-APCI. While such matrix effects with cholesterol incorporation are clearly significant, an extensive study is hampered by the rapid clogging of the MS inlet even at the ultimately low cholesterol concentrations.

At 40% cholesterol, quantified DOPC then returns to lower levels. In the literature, at high levels of cholesterol incorporation, interactions between DOPC's acyl chains and cholesterol's steroid ring may confer rigidity to phospholipid membrane structure.[26] Such immobilization of the phospholipids by cholesterol decreases membrane permeability and may likewise inoculate against acoustic disruption. Conversely, at lower levels of cholesterol (≤10% mol) in the bilayer, cholesterol's presence have been associated with increased membrane fluidity.[27] Therefore, further optimization of the SAW disruption efficiency must take into account the cholesterol composition.

Finally, we had incidentally observed that the SAWN-APCI method demonstrated capability for small protein ionization under native conditions as similar techniques have previously.[28] In Figure 7A, we show the mass spectrum of sampled droplets containing 14 kDa cytochrome C and spiked DOPC lipid with formal concentrations of 12.5 and 25 μM, respectively, observed by SAWN-APCI alone. In Figure 7B,

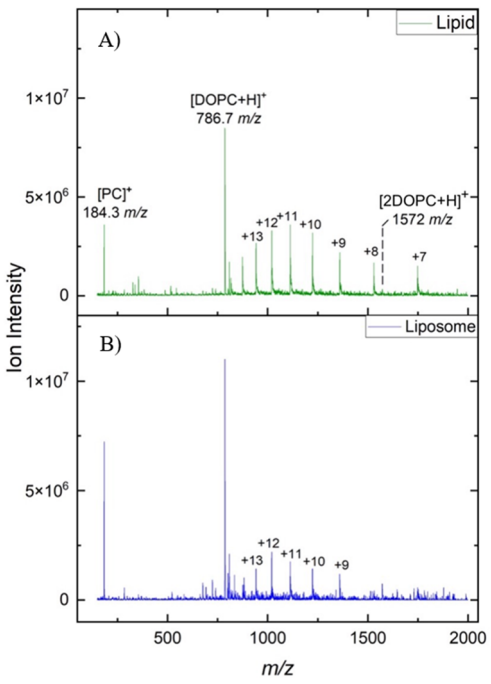

Figure 7. (a) Mass spectrum of solutions combining the DOPC lipid with cytochrome C subjected to SAWN-APCI alone. (b) Mass spectrum of DOPC liposome with free cytochrome C present, after being subjected to both SAW disruption and SAWN-APCI.

the cytochrome C is spiked into the DOPC liposome solution (not incorporated into the liposomes themselves), which is then subjected to 40 s of 64 MHz SAWs prior to SAWN-APCI. Cytochrome C signal is still recovered but may be subtly influenced by the disruption phase. One feature of these spectra worth mentioning, the dominant charge states of +11 and +12 indicates relatively unfolded conformations of the cytochrome C. Additionally, regarding the DOPC lipid, headgroup signal is outsized in the liposome, suggesting some complex internal energy deposition. Evidence of such aqueous sampling is promising for applications using native conditions and warrants further investigation.

DISCUSSION

SAWN-APCI provides a similar signal to ESI and successfully ionizes both polar DOPC and nonpolar cholesterol, potentially mitigating matrix complications in lipidomics assays. SAWN-APCI by itself is primarily advantageous, as there is no narrow-bore emitter to clean and any potential lipid aggregates are dispersed during nebulization. High frequency SAWs have been shown to release DOPC lipids from liposomes even those including cholesterol. On the other hand, cholesterol incorporation results in matrix effects that ultimately impact disruption efficiency. Using DOPE as an internal standard, we attempted to assess the recovery and the efficiency of the disruption SAW by calibration. Across all liposomes, the recovered DOPC was higher than the initial DOPC concentration, such that implementation of the internal standard warrants further consideration.

Overall, liposomes systematically processed by acoustics reveal a promising mechanical alternative to chemical lysis. The methods explored support a broadband analysis using sustained (>30 s) high frequency (>64 MHz) disruption SAW without the use of chemical lysing agents. Liposomes down to

https://doi.org/10.1021/acs.analchem.3c01722
Anal. Chem. 2023, 95, 13497−13502

concentrations of 1.6 μM DOPC or ~11 × 10^6 liposomes/μL were detectable from 1 μL which may prove particularly beneficial for precious, low-volume samples and for potentially high-throughput applications. Additional studies showing the operation of SAWs on aqueous solutions are relevant to potential native mass spectrometry applications of higher order structures between lipids and proteins. Future work of the SAW technology may thus impact the study of lipid aggregates, extracellular vesicles, and lipid−protein complexes.

■ ASSOCIATED CONTENT

Supporting Information

The Supporting Information is available free of charge at https://pubs.acs.org/doi/10.1021/acs.analchem.3c01722.

> Sample solution preparation, depiction of SAW application in continuous mode, raw mass spectra of liposome-derived lipids with and without SAW disruption, representative infrared images and temperature spikes associated with SAW thermal evolution, and representative raw mass spectra of calibrator solutions and spiked liposome solutions containing internal standards (PDF)

■ AUTHOR INFORMATION

Corresponding Author

Theresa Evans-Nguyen − *Department of Chemistry, University of South Florida, Tampa, Florida 33620, United States;* orcid.org/0000-0001-7675-1060; Email: evansnguyen@usf.edu

Authors

Ashton N. Taylor − *Department of Chemistry, University of South Florida, Tampa, Florida 33620, United States*

Yuqi Huang − *Department of Chemical, Biological, and Materials Engineering, University of South Florida, Tampa, Florida 33620, United States*

Cheyenne Sircher − *Department of Chemistry, University of South Florida, Tampa, Florida 33620, United States*

Sandra Khalife − *Department of Chemistry, University of South Florida, Tampa, Florida 33620, United States*

Venkat Bhethanabotla − *Department of Chemical, Biological, and Materials Engineering, University of South Florida, Tampa, Florida 33620, United States;* orcid.org/0000-0002-8279-0100

Complete contact information is available at: https://pubs.acs.org/10.1021/acs.analchem.3c01722

Author Contributions

A.N.T.: Developed methods for disruption and nebulization processes; Prepared and analyzed all working samples; Wrote manuscript. C.S.: Optimized experimental methods including liposome synthesis and validation; Revised draft manuscript. Y.H.: Fabricated and tested SAW devices; Facilitated liposome disruption studies. S.K.: Synthesized DOPC and DOPC/cholesterol liposomes. V.B.: Oversaw SAW chip production and optimization. T.E.-N.: Oversaw experimental design for lipid and liposome studies; Revised draft manuscript.

Notes

The authors declare no competing financial interest.

■ ACKNOWLEDGMENTS

This work is supported by the National Science Foundation, Grant Number: 2108795. Table of Contents graphic is an original figure created with Biorender.com.

■ REFERENCES

(1) Large, D. E.; Abdelmessih, R. G.; Fink, E. A.; Auguste, D. T. *Adv. Drug Delivery Rev.* **2021**, *176*, 113851−113864.
(2) Colombo, M.; Raposo, G.; Théry, C. *Annu. Rev. Cell Dev. Biol.* **2014**, *30* (1), 255−289.
(3) Wang, J.; Wang, C.; Han, X. *Anal. Chim. Acta* **2019**, *1061*, 28−41.
(4) Frick, M.; Schwieger, C.; Schmidt, C. *Angew. Chem.* **2021**, *60* (20), 11523−11530.
(5) Frick, M.; Schmidt, C. *Chem. Phys. Lipids* **2019**, *221*, 145−157.
(6) Simpson, R. J.; Lim, J. W.; Moritz, R. L.; Mathivanan, S. *Expert review of proteomics* **2009**, *6* (3), 267−283.
(7) Koivusalo, M.; Haimi, P.; Heikinheimo, L.; Kostiainen, R.; Somerharju, P. *J. Lipid Res.* **2001**, *42* (4), 663−672.
(8) Yang, K.; Han, X. *Metabolites* **2011**, *1* (1), 21−40.
(9) Song, L.; You, Y.; Evans-Nguyen, T. *Anal. Chem.* **2019**, *91* (1), 912−918.
(10) Song, L.; You, Y.; Perdomo, N. R.; Evans-Nguyen, T. *Anal. Chem.* **2020**, *92*, 11072−11079.
(11) Sankaranarayanan, S. K. R. S.; Singh, R.; Bhethanabotla, V. R. *J. Appl. Phys.* **2010**, *108* (10), 104507.
(12) Li, S.; Bhethanabotla, V. R. *Sensors (Basel)* **2019**, *19* (18), 3876−3888.
(13) Taller, D.; Richards, K.; Slouka, Z.; Senapati, S.; Hill, R.; Go, D. B.; Chang, H.-C. *Lab Chip* **2015**, *15* (7), 1656−1666.
(14) Nsairat, H.; Khater, D.; Sayed, U.; Odeh, F.; Al Bawab, A.; Alshaer, W. *Heliyon* **2022**, *8*, e09394.
(15) Lombardo, D.; Kiselev, M. A. *Pharmaceutics* **2022**, *14* (3), 543.
(16) Alves, N. J.; Cusick, W.; Stefanick, J. F.; Ashley, J. D.; Handlogten, M. W.; Bilgicer, B. *Analyst* **2013**, *138*, 4746−4751.
(17) Marsh, D. *Handbook of Lipid Bilayers*; CRC Press, Inc.: Max-Planck-Institut für biophysikalische Chemie: Göttingen, Germany.
(18) Hauner, I. M.; Deblais, A.; Beattie, J. K.; Kellay, H.; Bonn, D. *J. Phys. Chem. Lett.* **2017**, *8*, 1599−1603.
(19) Prajapati, K.; Patel, S. *Arch. Appl. Sci. Res.* **2012**, *4* (1), 662−668.
(20) Esteban, B.; Riba, J.-R.; Baquero, G.; Puig, R.; Rius, A. *Fuel* **2012**, *102*, 231−238.
(21) Brown, R. E. *Biochim. Biophys. Acta* **1992**, *1113* (0), 375−389.
(22) Walczak, J.; Bocian, S.; Buszewski, B. *Food Analytical Methods* **2015**, *8*, 661−667.
(23) Shelley, J. T.; Wiley, J. S.; Chan, G. C. Y.; Schilling, G. D.; Ray, S. J.; Hieftje, G. M. *J. Am. Soc. Mass Spectrom.* **2009**, *20* (5), 837−844.
(24) Briuglia, M.-L.; Rotella, C.; McFarlane, A.; Lamprou, D. A. *Drug Delivery and Transl. Res.* **2015**, *5*, 231−242.
(25) Haberland, M. E.; Reynolds, J. A. *Proc. Natl. Acad. Sci. U. S. A.* **1973**, *70* (8), 2313−2316.
(26) Mainali, L.; Feix, J. B.; Hyde, J. S.; Subczynski, W. K. *Journal of Magentic Resonance* **2011**, *212*, 418−425.
(27) Subczynski, W. K.; Pasenkiewicz-Gierula, M.; Widomska, J.; Mainali, L.; Raguz, M. *Cell Biochem. Biophys.* **2017**, *75* (3−4), 369−385.
(28) Marcus, R. K.; Hoegg, E. D.; Hall, K. A.; Williams, T. J.; Koppenaal, D. W. *Mass Spectrom. Rev.* **2023**, *42*, 652−673.